Dual-Emission Band All-Fiber Laser based on Theta Cavity with Thulium- and Holmium-Doped Fibers

Svyatoslav Kharitonov*, Camille-Sophie Brès
Ecole Polytechnique Fédérale de Lausanne (EPFL), Photonic Systems Laboratory (PHOSL), STI-IEL, Station 11, CH-1015 Lausanne, Switzerland
**svyatoslav.kharitonov@epfl.ch*

Abstract: We present first dual-wavelength all-fiber laser, based on isolator-free theta cavity with two fiber Bragg mirrors and thulium- and holmium-doped fibers. Laser provides 350mW total power with 8% slope efficiency, and linewidth less than 0.1nm.
OCIS codes: (060.3510) Lasers, fiber; (060.2390) Fiber optics, infrared; (160.5690) Rare-earth-doped materials

1. Introduction

A rapid development of fiber laser (FL) sources near 2 µm, based on transitions in thulium and holmium trivalent cations, Tm^{3+} and Ho^{3+} respectively, is motivated by their various applications in spectroscopy and ranging [1], material and biological tissues processing [2], telecommunications [3], and nonlinear optics [4]. For wavelength selection, ring cavity FL configurations require a band-pass filtering element (grating, Fabry-Pérot etalon etc.). Moreover, optical isolators that ensure a unidirectional lasing generally have a limited operational bandwidth of few hundreds of nm. If the FL operates in Fabry-Pérot type resonator, a matched fiber Bragg grating (FBG) pair should be used. Alternatively, isolator-free unidirectional ring fiber cavity ("theta" or "yin-yang" resonator [5]) represents a cost-effective solution. In theta cavities, non-reciprocal losses are introduced by providing an S-shape feedback within the main ring. A core-pumped continuous wave thulium-doped FL (TDFL) that provides sub-Watt output power with a slope efficiency of 25%, 250 nm tuning range, and linewidth of 0.2 nm, was recently demonstrated by our group [6]. The TDFL wavelength was tuned by fiberized grating filter. A high power Q-switched theta cavity TDFL using carbon nanotube saturable absorber was also shown [7]. Moreover, we reported truly all-fiber narrow linewidth unidirectional ring TDFL, relying on theta cavity and FBG as wavelength selective element. The laser output power in the latter case reached 1 W, with 30% slope efficiency and spectral width less than 0.22 nm [8].

In this paper, we present a modified theta cavity laser with FBG enabling dual-emission bands. Both thulium- and holmium-doped silica fibers are incorporated in the cavity, providing a narrow-linewidth emission at 2100 nm, and in some configurations additionally at 1950 nm, while being pumped with a single source at 1600 nm. The output power up to 350 mW with 8% slope efficiency is achieved, and can be further improved by optimizing the doped fiber length, and reducing absorption and bending losses in passive components in 2100 nm band.

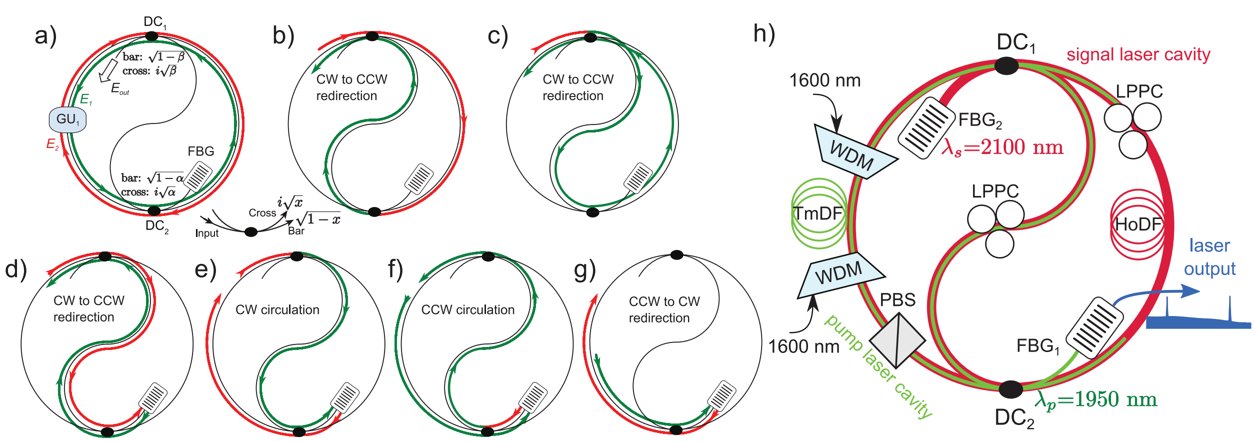

Fig. 1. (a)-(g) Single wavelength theta cavity with FBG layout. Optical path, not affected by FBG: a) Main paths for the clockwise (CW – red) and the counter –clockwise (CCW – green) propagating modes, corresponding to a ring; b-c) two possible rectifying paths, redirecting the CW modes towards the CCW modes. Optical path, influenced by FBG: d) CW to CCW redirection; e) CW circulation; f) CCW circulation; g) CCW to CW redirection. (h) Experimental implementation of dual-emission bands fiber laser with thulium- and holmium-doped fibers (TmDF and HoDF, respectively): WDM – wavelength division multiplexer; LPPC – large paddle polarization controller, PBS – polarization beam splitter

978-1-943580-23-1/17/$31.00 ©2017 Optical Society of America

2. Principles of operation and fiber laser implementation

The main idea behind theta resonator is of lasing direction rectification by introducing non-reciprocal cavity losses using S-shape feedback, as described in details in [6]. We consider a ring resonator that consists of a lumped gain unit GU_1, and two directional couplers, which cross-outputs are connected together to form the S-shape feedback (Fig. 1). Thus, the theta cavity is essentially two overlapped Sagnac loops. E_1 and E_2 are counter-clockwise (CCW) and clockwise signals entering the amplifying unit. One of the unused ports of the directional couplers can be cleverly exploited by connecting a FBG. If no FBG is present in the design, only three possible paths are sustained: CCW and CW circulation in the main ring (Fig. 1a), and two rectifying paths from CW to CCW modes (Fig. 1b-c). If a FBG is connected to the free port of directional coupler 2 (DC_2), one obtains four extra paths, involving the grating: CW to CCW redirection, CW circulation, CCW circulation, and CCW to CW redirection (Fig. 1d-g). Therefore, the laser spectral line shape can be controlled by the FBG in reflection mode, which provides a wavelength selective feedback in the cavity.

The cavity functionality can be enhanced toward dual-emission band operation, by adding the second gain unit (GU_2) to the main ring, and corresponding FBG to the last unused port of the directional couplers, as shown in Fig. 1h. In the presented configuration, GU_1 consists of 11.5 m of thulium doped fibre (TmDF, TmDF200, OFS Fitel Denmark ApS) bi-directionally core pumped with a 1600 nm pump obtained from an amplified tunable laser source. FBG_1 is chosen to select 1950 nm wavelength. GU_2 consists of 1.7 m of holmium-doped fibre (HoDF, SM-HDF-10/130, Nufern) core pumped with 1950 nm emission of GU_1. FBG_2 is centered at 2100 nm. So, GU_1 functions in a Sagnac loop cavity, acting as a pump source for GU_2, which operates in the conventional theta cavity. By adjusting the FBGs reflectivity, and $DC_{1,2}$ coupling ratio, we can obtain either single-wavelength emission at 2100 nm, or dual-wavelength emission at both 2100 nm, and 1950 nm. As the presented laser is envisioned as polarized light source, the polarization beam splitter (PBS) and large paddle polarization controllers (LPPC) are optionally included in the cavity. DC_1 and DC_2 have cross-coupling ratios of 25% and 90%, respectively. The power reflection coefficient of the grating, used as FBG_1, is 99% and 13.5% for the single- and dual-wavelength operation, respectively. The FBG_2 has 0.2 nm FWHM bandwidth and 95% peak reflection. The transmission port of FBG_1 is used as a laser output in both configurations.

3. Results and discussion

First, the single-wavelength operation at 2100 nm was investigated, and the results are summarized in Fig. 2. The laser provides up to 300 mW output power with 8% slope efficiency, threshold power of 1.4 W (Fig. 2a), and OSNR better than 55 dBm/1nm (Fig. 2b). Remarkably, the laser linewidth (FWHM) is virtually constant at 0.1 nm, and stabilizes versus increasing pump power, which is indicated by lowering the wavelength jitter $\Delta\sigma_\lambda$ (Fig. 2b-c). It should be noted that despite of a high reflection (HR) of FBG_1 (99%), there is a very small residual 1950 nm signal in output spectra (Fig. 2c). A spectral instability of the 1950 nm signal is caused by 1.5 nm broad reflection bandwidth of HR grating.

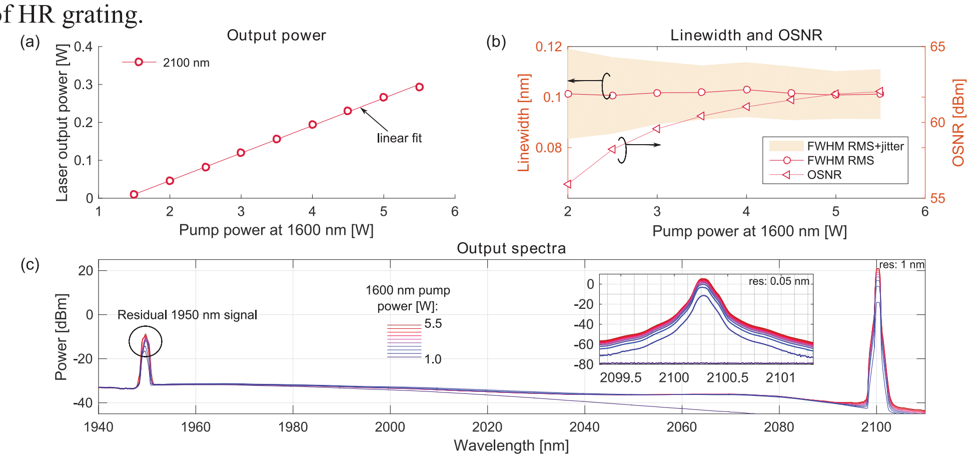

Fig. 2: Single-wavelength laser performance characteristics: a) Output power vs. pump power, b) Laser linewidth (FWHM) and OSNR vs. pump power. Possible fluctuations of FWHM (linewidth jitter $\Delta\sigma_\lambda$) are shown as well (shaded area). The method of evaluation of $\Delta\sigma_\lambda$ has been described in [6]; c) Output laser spectra, recorded at low and high (insets) resolution for various levels of the pump power.

Furthermore, changing the FBG_1 to the low-reflection (LR) grating with 0.1 nm FWHM bandwidth and 13.5% peak reflection, we obtain a dual-band fiber laser operation, where 1950 nm emission from GU_1 is partly coupled out, and partly forwarded as a pump for the holmium-doped fiber in GU_2. The laser performance characteristics are shown in Fig. 3. As the FBG_1 reflectivity has been reduced, the loss of Sagnac resonator at 1950 nm is increased, resulting in a lower power, coupled to GU_2, and, consequently, in lower power generated at 2100 nm (up to 220 mW with 6% slope efficiency, and 1.5 W threshold power), while the OSNR remain higher than 55 dB/1nm. The 1950 nm signal evolves nonlinearly with increasing 1600 nm power, reaching a maximum value of 150 mW (Fig. 3a). Lower OSNR of 1950-nm signal comparing to 2100-nm one (42-50 dB/1nm) can be explained by the fact that GU_1 operates at the peak of TmDF gain spectrum (Fig. 3b-c). The laser linewidth is stabilized at about 0.07 nm and 0.09 nm FWHM for 1950 nm and 2100 nm signals, respectively (Fig. 3b).

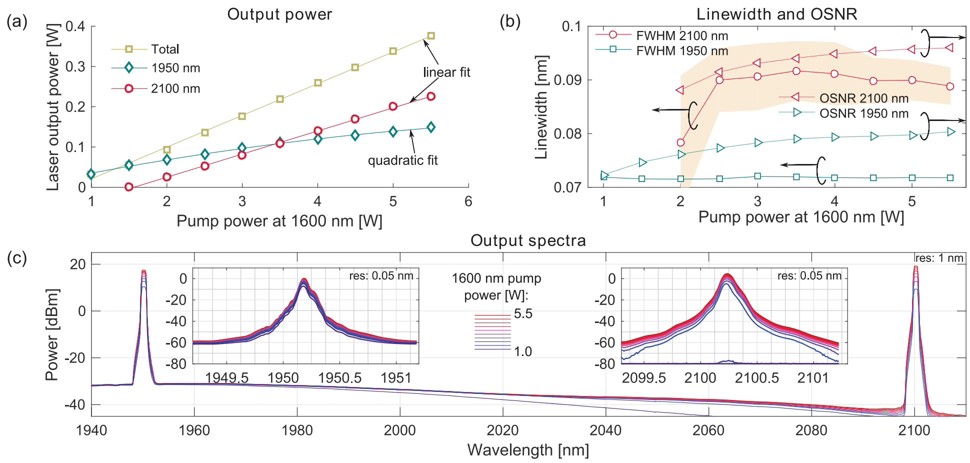

Fig. 3: Dual-wavelength laser performance characteristics: a) Output power vs. pump power, b) Laser linewidth (FWHM) and OSNR vs. pump power. The shaded area depicts the linewidth jitter of 2100 nm laser c) Output laser spectra, recorded at low and high (insets) resolution for various levels of the pump power.

A high lasing threshold at 2100 nm in both configurations can be attributed to relatively high cavity loss, introduced by some components (PBS, LPPC), a redundant length of TmDF (11.5m), and bending and absorption loss in passive fibers. So, performance of 2100 nm laser can be significantly improved by an optimization of the resonator. The bending losses can be reduced after replacement of passive components made with SMF-28 fiber, by ones based on SM2000 fiber. An overall shortening of cavity length will reduce an absorption in a fused silica (0.1 dB/m at 2100 nm). Finally, the optimum coupling ratios of DC_1 and DC_2 have to be determined by simulations to balance the losses of GU_1 and GU_2 resonators: so, increasing the cross-coupling ratio of DC_1 improves the performance of GU_1 in Sagnac resonator, while increasing the losses in theta resonator for GU_2. The proposed laser configuration can be used as a master oscillator, where pump and signal are generated in the same cavity. Alternatively, the laser could provide both parametric pump and seed for four-wave mixing experiments beyond 2 μm in low-phonon energy fibers [4]. Moreover, the dual-band emission can be stimulated on different transitions in the same gain medium. For example, ${}^3H_4 \rightarrow {}^3F_4$ transition in thulium-doped fluoride at 1460 nm is self-terminated, so cooperative lasing at the transition ${}^3F_4 \rightarrow {}^3H_6$ (1900 nm) is required to deplete the ${}^3F_4$ level.

This work is supported in part by the SNSF under grant agreement 200021_140816 and the Swiss Space Center/European Space Agency (ESA).

4. References

[1] S. Ishii et al, "Coherent 2 μm differential absorption and wind lidar with conductively cooled laser and two-axis scanning device," Appl. Opt. **49**, 1809–1817 (2010).
[2] S. D. Jackson, "Towards high-power mid-infrared emission from a fibre laser," Nat. Photonics **6**, 423–431 (2012).
[3] M. N. Petrovich et al, "Demonstration of amplified data transmission at 2 μm in a low-loss wide bandwidth hollow core photonic bandgap fiber," Opt. Express **21**, 28559–28569 (2013).
[4] S. Xing et al, "Characterization and modeling of microstructured chalcogenide fibers for efficient mid-infrared wavelength conversion," Opt. Express **24**, 9741-9750 (2016).
[5] Y. H. Ja, "Densely spaced two-channel wavelength division demultiplexer with an S-shaped two-coupler optical fiber ring resonator," Appl. Opt. **32**, pp. 6679–83 (1993).
[6] S. Kharitonov and C.-S. Brès, "Isolator-free unidirectional thulium-doped fiber laser," Light Sci. Appl. **4**, e340 (2015).
[7] M. Chernysheva et al, "High Power Q-Switched Thulium Doped Fibre Laser using Carbon Nanotube Polymer Composite Saturable Absorber," Sci. Rep. **6**, p. 24220 (2016).
[8] S. Kharitonov and C.-S. Brès, "Unidirectional all-fiber thulium-doped laser based on theta cavity and fiber Bragg grating as filtering element," Advanced Solid State Lasers Conference, AM5A.5 (2016).